Ecosystems (2003) 6: 384–398
DOI: 10.1007/s10021-002-0191-8

ECOSYSTEMS

Spatial Patterns of Biomass and Aboveground Net Primary Productivity in a Mangrove Ecosystem in the Dominican Republic

Ruth E. Sherman,[1]* Timothy J. Fahey,[1] and Pedro Martinez[2]

[1]*Department of Natural Resources, Cornell University, Fernow Hall, Ithaca, New York 14853, USA;* [2]*Instituto Nacional de Recursos Hidraulicos, PROMASIR, D.N. Apartado Postal 1407, Santo Domingo, Dominican Republic*

Abstract

The objective of this study was to quantify spatial patterns in above- and belowground biomass, primary productivity, and growth efficiency along a tidal gradient in a 4700-ha mangrove forest in the Dominican Republic. We tested the hypothesis that spatial patterns of forest structure and growth following 50 years of development were associated with variations in the soil environment across the tidal gradient. Twenty-three plots were monitored from 1994 to 1998. Aboveground biomass and biomass accumulation were estimated by applying allometric regression equations derived from dimension analysis of trees harvested at our study site. Soil porewater salinity ranged from 5 to 38 $g \cdot kg^{-1}$ across the tidal gradient, and most measurements of forest biomass and productivity were inversely related to salinity. Mean standing biomass (233 ± 16.0 $Mg \cdot ha^{-1}$; range, 123.5–383.5), biomass increment (9.7 ± 1.0 $Mg \cdot ha^{-1} y^{-1}$; range, 3.7–18.1), annual litterfall rates (11.4 $Mg \cdot ha^{-1}yr^{-1}$; range, 10.2–12.8), leaf area index (LAI) (4.4 $m^2 \cdot m^{-2}$; range, 2.9–5.6), aboveground net primary productivity (ANPP) (19.7 $Mg \cdot ha^{-1} y^{-1}$; range, 15.6–25.0), and growth efficiency (1.6± 0.2 $kg \cdot ha^{-1}y^{-1}$; range, 1.0–3.6) all showed an inverse linear relationship with salinity. Fine-root biomass (≤ 2 mm) (9.7 ± 1.2 $Mg \cdot ha^{-1}$; range, 2.7–13.8) showed a weak tendency to increase with salinity, and the ratio of root to aboveground biomass increased strongly with salinity. Our results suggest that physiological stresses associated with salinity, or with some combination of salinity and other covarying soil factors, control forest structure and growth along the tidal gradient. The higher allocation of carbon to belowground resources in more saline sites apparently contributed to reductions in ANPP along the tidal gradient.

Key words: mangrove forests; biomass; primary productivity; growth efficiency; tidal gradient; salinity; environmental stress; species composition; Dominican Republic.

Introduction

One of the greatest challenges in ecology today is determining the causes and consequences of spatial variability in ecosystem structure and function (Carpenter and Turner 1998). Mangrove forests, the dominant ecosystem of sheltered coastlines

Received 10 September 2001; accepted 16 September 2002; published online May 20, 2003.
*Corresponding author; e-mail: res6@cornell.edu

throughout tropical and subtropical regions of the world, occur in a diversity of environmental settings, and their structural and functional characteristics vary tremendously at global, regional, and local scales. On a global scale, temperature is the dominant control on the structural development and growth of mangrove forests. Standing biomass and tree height are at a maximum in the humid tropics and decline progressively with increasing latitude to about 35°N and 38°S, where mangroves are replaced by salt marsh ecosystems (Saenger and Snedaker 1993). Owing to limited data; the relationship between patterns of productivity and latitude is not as clear; however, a similar pattern of decreasing productivity with increasing latitude has been observed in mangrove forests along the eastern coast of Australia (Clough 1992).

Within a climatic zone, the structural development and growth of mangrove forests are controlled largely by the geomorphic characteristics of the coastal landscape (Thom 1982). Hydrological processes, such as tidal activity, waves, river discharge, and freshwater inputs, have a particularly strong influence on the chemical and physical conditions in mangrove ecosystems. As a result, the structure, composition, and function of these communities are closely linked to their geomorphologically defined habitats (Thom 1967, 1982; Wolanski and others 1992; Woodroffe 1992). The most extensive and structurally complex mangrove forests develop in deltas of low relief and high tidal amplitude that receive abundant supplies of freshwater and nutrients, such as the delta of the Orinoco River in Venezuela and the deltas of the Ganges and Brahmaputra rivers in the Bay of Bengal. At the other extreme are small isolated stands that develop in reef environments on coral rubble or sand; these mangrove forests often are dominated by a single species, attain canopy heights of only a few meters, and are nutrient-poor (Woodroffe 1992).

At local scales, spatial patterns of composition, biomass, and productivity are probably controlled primarily by soil factors and disturbance history (Smith 1992; Ellison and Farnsworth 1993; McKee 1995b; Chen and Twilley 1999). Patterns of tidal inundation, overland runoff, and groundwater seepage all influence physical–chemical soil characteristics, creating environmentally complex gradients across the landscape (Twilley 1995). Considerable effort has been expended to identify species distribution patterns and determine the mechanisms underlying the often striking spatial patterns in mangrove forests. Species distribution patterns within mangrove landscapes have been attributed to the responses of individual species to soil edaphic factors, such as tidal inundation, salinity, soil sulfide concentrations, and soil redox potential, as well as biotic influences, such as herbivory, seed predation, and competition, all of which can vary across the tidal zone (reviewed by Smith 1992). Few studies have documented the spatial variability of ecosystem processes, such as primary productivity. Both salinity (Imbert and others 2000) and soil nutrient availability (Day and others 1987; Chen and Twilley 1999) have been implicated as the principal factors that regulate patterns of mangrove forest structure and productivity; however, conclusive results that would define environmental controls have been difficult to obtain because of the complex disturbance history in these areas and the consequent overriding effects of stand age on forest production and growth (Ryan and others 1997; Chen and Twilley 1999).

The Samaná Bay mangrove forest in the Dominican Republic, the site of this long-term study on forest dynamics, is an ideal setting to evaluate the environmental controls on mangrove forest development and productivity. The forest is largely even-aged, having originated after a devastating tidal wave in 1946 (Sachtler 1973; Alvarez and Cintrón 1984; Sherman and others 2000). Since 1994, we have been monitoring 23 permanent plots that extend across 5 km of this 4700-ha forest. Species composition and soil environment vary across the tidal gradient (Sherman and others 1998, 2000), and we expected that forest biomass and productivity in this ecosystem also would change along the tidal gradient. The objective of the present study was to quantify spatial patterns in biomass, productivity, and growth efficiency in relation to soil factors that vary across the tidal gradient. We hypothesized that productivity, biomass, and growth efficiency would increase with decreasing salinity along the tidal gradient from coastal to inland sites as a consequence of reduced environmental stress and changing species composition.

Methods

Study Site

The study was conducted in a mangrove forest located at the western end of Samaná Bay in the Los Haitises National Park, Dominican Republic, in the broad delta created at the months of the Yuna and Barracote rivers (19°10'N, 69°40'E) (Figure 1). The forest is dominated by the red mangrove (*Rhizophora mangle* L., Rhizophoraceae) and the white mangrove (*Laguncularia racemosa* [L.] Gaertn., Combretaceae), with a small proportion of black man-

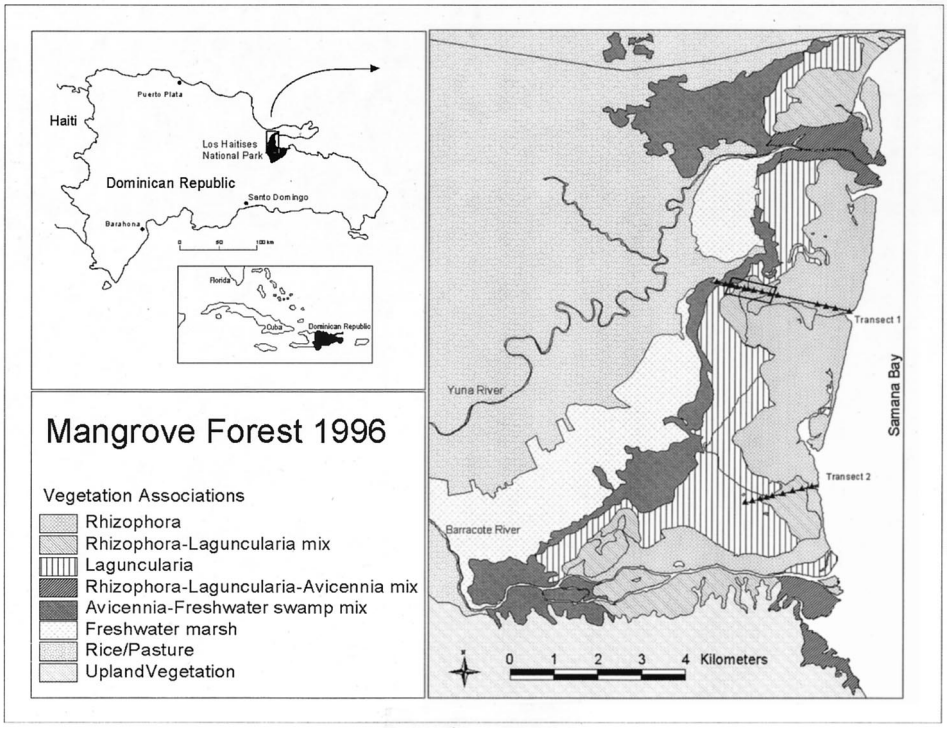

Figure 1. Map of the mangrove forest study area in the Los Haitises National Park, Dominican Republic, showing the mangrove forest community associations and the transects (*solid lines*) and plots (*triangles*) used for field sampling. Litterfall was measured in a subset of eight plots along transect 1 (indicated by the rectangle).

grove (*Avicennia germinans* L., Avicenniaceae). A freshwater swamp, a cattail marsh, and an extensive rice production region form the inland border of the mangrove forest. A tidal wave destroyed much of the forest in 1946 (Sachtler 1973; Alvarez and Cintrón 1984), and most of the current forest arose since that time. Thus, its approximate age was 50 years at the time of the present study. Hurricane Georges, a category three hurricane on the Saffir-Simpson scale, hit the Dominican Republic in September 1998 (Pasch 1999), causing extensive damage to the mangrove forest (Sherman and others 2001). Therefore our report is based on data collected between January 1994 and January 1998.

Mean annual temperature is 26.3°C. Rainfall averages 2065 mm per year; in the driest months (February and March), it averages 100 mm per month (Oficina Nacional de Meteorologia, Dominican Republic). Mean tidal amplitude is approximately 0.6 m. The soils have been field-classified as fine–silty isohyperthermic Typic Hydraquents. Throughout most of the mangrove forest, the soil was characterized by an organic peat mat approximately 30–50 cm in thickness, underlain by a highly decomposed organic layer about 1 m in thickness. The peat mat consisted primarily of live roots, whereas the deeper organic soil layer contained few living roots. Underlying the organic soil was a firm clay substrate. The peat mat was absent nearer the coast, where the soil was predominantly an allochthonously derived silty–clay marl that extended approximately 250 m inland. At the upland margin of the forest, the clay layer came to the surface and the organic peat mat was absent.

Plot Surveys and Environmental Measurements

To characterize the composition, structure, and spatial pattern of the forest and determine their relationship to environmental features, we established permanent plots along two transects that traversed the mangrove ecosystem (Figure 1). One transect extended 3.1 km from the coast inland to the transition to freshwater marsh; the second transect extended from the coast inland for 1.8 km. Thirteen plots were established along transect 1 and nine plots along transect 2. To estimate stem density and basal area, all trees greater than 5 cm in diameter at breast height (dbh) were measured and tagged in each 30-m diameter plot. On *R. mangle* trees, stem diameter measurements were made above the highest prop root, but we refer to these measurements as dbh. The dbh of each tree was remeasured every 2 years and mortality recorded. The heights of the four tallest canopy trees were measured in each plot using a clinometer. In addition, the heights of 171 trees located throughout the forest were measured to develop dbh versus height relationships for the three species.

Soil water samples were collected from each of

the permanent plots on eight different dates over a 3-year period (1995–97) at both high and low tide for analysis of salinity and nutrients. Surface water samples were collected by withdrawing standing water from the soil surface with a 50-ml syringe. Soil porewater samples were collected from zero-tension lysimeters placed at a depth of approximately 0.5 m (Sherman and others 1998). All samples were filtered immediately after collection using 0.45-μm syringe filters. Salinity, total dissolved nitrogen (TN), and total dissolved phosphorus (TP) were measured on all samples. Salinity was measured using a Leica model 10423 refractometer. Samples for TP and TN were oxidized in a combined persulfate digestion method (Grasshoff and others 1983). TP was subsequently analyzed on a Beckman DU 50 spectrophotometer using the molybdate colorimetric assay; TN was analyzed on a continuous flow analyzer using the phenol-nitroprusside method. A subset of the samples was analyzed for soluble reactive phosphorus (SRP), organic P, nitrate (NO_3^-), ammonium (NH_4^+), and organic nitrogen (N). These samples were carried to Ithaca, New York, without freezing and analyzed within a week of collection.

Soil samples were collected to a depth of 30 cm from each plot in December 1994 using a 50-cm length of 8-cm diameter polyvinylchloride (PVC) pipe held together with hose clamps. Soil samples were air-dried and transported to Ithaca, New York, for analysis. For P fractionation, we used a modified sequential extraction scheme developed by Jensen and Thamdrup (1993) for marine sediments. We measured three major soil P pools: reactive or mobile P (loosely sorbed SRP, iron (Fe)-bound P pools, SRP from clay minerals and oxides, and hydrolyzable organic P), calcium-bound P (Ca-P), and refractory organic P. In a major modification to the original scheme, we extracted all of the reactive P in one step. Because we dried our soil samples, it was not possible to quantify separate reactive P pools as described by Jensen and Thamdrup (1993) (H. S. Jensen personal communication).

In the first step, soil samples were shaken in 0.1-M NaOH for 18 h to extract the reactive P fraction. The suspension was then centrifuged and analyzed for TP and SRP. Organic P was defined as the difference between TP and SRP. In step two, the samples were shaken for 2 h in 0.5-M HCl to extract Ca-P. In the final step, the soil was ashed and then boiled for 10 min in 1-M HCl to extract refractory organic P pools. SRP was analyzed in the extracts of steps two and three.

Aboveground Biomass and Biomass Increment

Aboveground biomass and biomass increment were estimated for each plot using standard allometric approaches (Whittaker and Woodwell 1968; Whittaker and others 1974). Best-fit allometric equations for biomass components were developed for each species by destructive harvest; these equations were applied to the plot survey on a tree-by-tree basis. Twenty-four trees, ranging in size from 10 to 30.4 cm in dbh, were destructively harvested at our study site to develop the allometric relationships for estimating individual tree biomass. After the trees were felled, total height was measured, and the branches were cut from the main stem. The moist weight of all branches, leaves, twigs, and prop roots (*R. mangle* only) was measured in the field. Subsamples of all components were taken to the laboratory, dried to constant mass at 70°C, and reweighed to obtain the moisture content of the various biomass components. The weight of the main stem was estimated from field measurements of trunk volume and laboratory measurements of wood density. The density of the wood for each species was estimated by removing a stem cross section approximately 5 cm in thickness. The sections were taken to the laboratory, where the volume of each section was measured and dried to constant mass, and the ratio of moist volume to dry weight was determined.

Finally, the leaf area index (LAI) in each plot was estimated from leaf biomass estimates and leaf area-to-weight ratios for each species. A subsample of about 50 leaves of each species was collected at random from the harvested trees and placed in a plant press at the field site. In the laboratory, the area of each leaf was determined using a Licor model LI-3100 leaf area meter, and the dry weight of each leaf was measured to ± 0.1 mg to establish the ratio of leaf area to weight for each species. To obtain the LAI (leaf area [m^2]/ground area [m^2]), the total leaf biomass of each tree, estimated from allometric equations, was multiplied by the ratio of leaf area to weight and summed for each plot. (Whittaker and Woodwell 1968).

Litterfall

Six 0.25-m^2 litterfall traps (Hughes and others 1987) were placed randomly in each of seven plots along the upper portion of transect 1 (Figure 1). Litterfall was collected in the upper tidal region only, due to logistical considerations of accessibility. However, this portion of the transect included all four of the forest community types identified at our

site (Sherman and others 2000) and traversed a wide range of salinities (1–22 g kg^{-1} surface water and 24–38 g kg^{-1} soil porewater). Litter was collected monthly or bimonthly between November 1995 through December 1997. Unfortunately, samples were not available in the summer and fall of 1996. Litter from each trap was separated by species into leaves, flowers, seeds, and woody material; it was then dried to constant mass at 70°C, and weighed.

Root Biomass

Root biomass was measured using soil cores taken from a subset of 10 plots along the upper part of transect 1. A stratified random sampling approach was employed to accommodate extremes of variation in soil substrate and root density. Three categories of soil substrate were classified visually: (a) open water containing few or no roots, (b) firm peat mat characterized by a compact root system, and (c) transitional zones between open water and firm peat. A line intercept method (Canfield 1941) was used to determine the area of each plot in these three soil type categories. Line transects were run in the cardinal directions (N–S and E–W), and the proportion of the transect intersecting each of the substrate types was measured. For each plot, the total transect length was 120 m.

To measure root biomass, 20 soil cores were collected from each of the plots; 10 cores were collected from random locations in the firm peat mat, and 10 cores were taken from the intermediate transitional substrate (the open water had few or no roots and was therefore excluded). The soil cores consisted of a 50-cm length of 8-cm–diameter PVC pipe held together with hose clamps and sharpened on the cutting end. Roots were sampled to a depth of 30 cm, transferred into labeled plastic bags, and kept cold until processed. Roots were separated into two size classes, 2 mm or less and 2–20 mm in diameter. Because it was difficult to sort out the dead roots, all roots (live and dead) were measured. The roots were cleaned, dried to a constant weight, and weighed. Large roots (more than 20 mm) were not sampled. The total dry weight of the roots (20 mm or less) was estimated on a plotwide basis by weighting the root density values in each soil surface category in each plot according to the estimated area of the plots in each of the three substrate categories.

Statistics

Pearson product moment correlation coefficients and linear regression models were used to determine the relationship between environmental factors and measures of forest structure and growth. One-way analysis of variance (ANOVA) was used to test for differences in biomass and measures of productivity among species and stand types. Two-way ANOVAs were used to analyze for differences and interactions in soil solution chemistry collected in different years and at different soil depths.

Results

Forest Structure and Soil Characteristics

The structural characteristics of the forest have been described in detail elsewhere (Sherman and others 2000); therefore, we will provide a brief summary only. *Rhizophora mangle* dominated the coastal sites along both transects, with composition shifting to a *Laguncularia racemosa*–dominated forest at the more inland sites (Figure 2a). *Avicennia germinans* became dominant at the inland forest margin along transect 1. Basal area ranged from 9.3 to 41.1 m^2 ha^{-1}, averaging 26.8 m^2ha^{-1} across all plots, and was greatest in the more inland *L. racemosa*–dominated plots. Tree density (at least 5 cm dbh) ranged from 170 to 1400 stems ha^{-1} (average, 1016). Density decreased along transect 1 from the coast inland but increased along transect 2. Tree height averaged 24 m across all plots, with maximum heights of 30 m in the more inland sites.

Surface water salinity decreased from the coast inland along both transects (Figure 3a). Surface water salinity averaged 13.0 ± 2.3 g kg^{-1} across all plots and ranged from 0.8 to 30.0 g kg^{-1}. Soil porewater salinity was significantly greater ($P < 0.001$) than surface water salinity; it ranged from 4.5 to 38.0 g kg^{-1} (average, 28.0). Along transect 1, soil porewater salinity decreased abruptly near the edge of the forest at 2700 m inland, whereas salinity declined more gradually across transect 2. There were no significant differences in salinity among collection dates ($P = 0.95$).

Concentrations of TN averaged 3.28 ± 0.23 mm L^{-1} in the surface water and 2.69 ± 0.77 mm L^{-1} in the soil porewater across all plots and dates (Figure 3b). Concentrations were significantly higher in 1995 than in 1996 ($P < 0.001$); they averaged 6.5 ± 0.45 and 5.6 ± 1.58 mm L^{-1} in the surface water and soil porewater, respectively, in 1995 and 0.11 ± 0.011 and 0.27 ± 0.063 mm L^{-1} in 1996. However, no significant differences were detected in concentrations between depths ($P = 0.67$) or interaction between year and depth ($P = 0.53$). Total N concentrations increased across the tidal gradient along transect 1 but did not change in a consistent

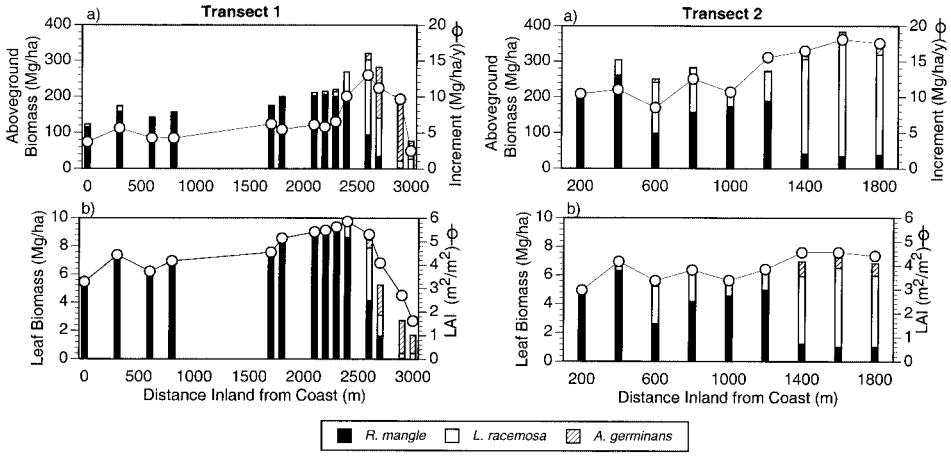

Figure 2. (**a**) Aboveground biomass and biomass increment and (**b**) leaf biomass and leaf area index (LAI) of trees (5 or more cm dbh) measured in plots along two transects across the tidal zone of a mangrove forest in the Dominican Republic. The overall height of the bar represents the total biomass of a plot; the segments represent individual species' contribution to the total. Biomass increment and LAI, represented by the line, are totals for each plot. Error bars are SEM from eight collection dates.

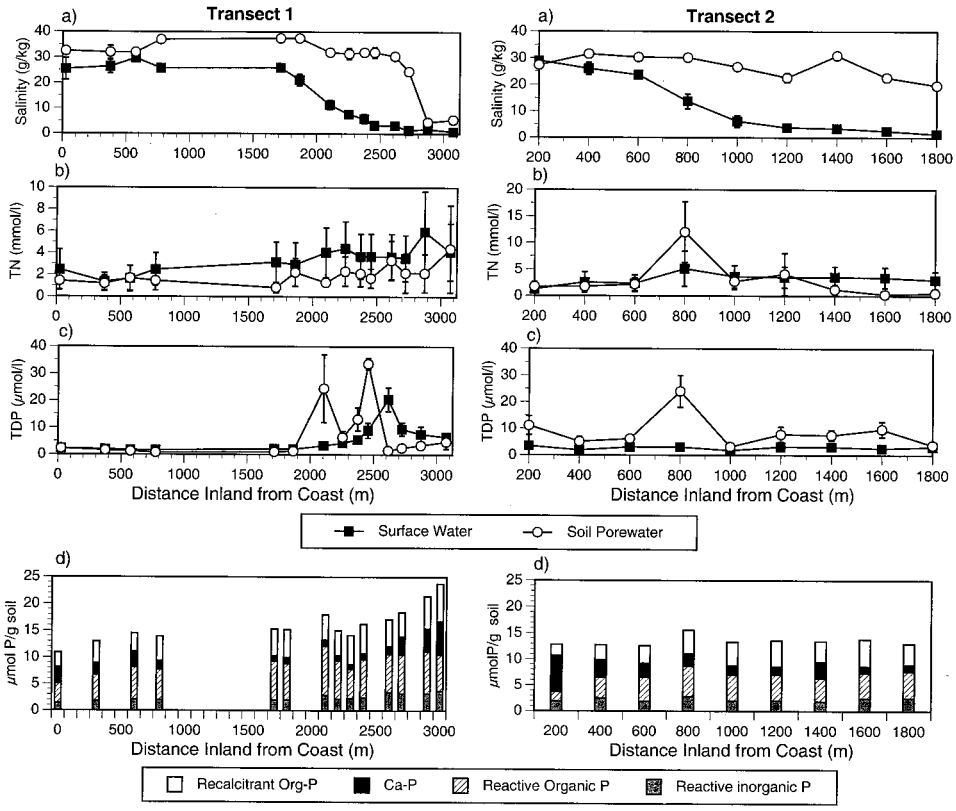

Figure 3. Changes in (**a**) salinity, (**b**) total nitrogen (TN), and (**c**) total dissolved phosphorus (TP) measured in the surface water and soil porewater (50-cm depth), and (**d**) concentrations of soil phosphorus (P) fractions measured in plots along two transects across the tidal zone of a mangrove forest in the Dominican Republic. The overall height of the bar represents total concentrations in the soil; segments represent the concentrations of the different fractions measured in each plot. Org = P, organic phosphorus; Ca-P, calcium-bound P; Pi, reactive inorganic P.

manner along transect 2. There was a strong inverse linear relationship of surface water TN concentrations with surface water salinity ($r = -0.71$, $P < 0.001$). Nitrate was negligible in all samples, whereas NH_4^+ accounted for 2%–30% of total N. Concentrations of NH_4^+ were not significantly different between years ($P = 0.35$) or depths ($P = 0.10$) and averaged 0.07 ± 0.03 mm L^{-1}.

Concentrations of TP averaged 4.47 ± 0.87 µm L^{-1} in the surface water and 7.68 ± 1.81 in the soil porewater (Figure 3c). SRP accounted for over 90% of TP in all samples, and TP and SRP concentrations

Table 1. Allometric Regression Equations of Various Components of Aboveground biomass on Parabolic Volume (PV) for Three Species of Mangrove Trees Harvested in the Los Haitises National Park, Dominican Republic

Species	Regression Equation	r^2 value
Rhizophora mangle		
(n = 8; size range, 10.1–30.4 cm dbh)		
Total biomass	$0.540\times PV^{1.117}$	0.97
Leaf biomass	$0.287\times PV^{0.998}$	0.86
Trunk biomass	$0.435\times PV^{1.074}$	0.96
Branch biomass	$0.145\times PV-6.69$	0.99
Prop root biomass	$0.317\times PV-24.98$	0.97
Laguncularia racemosa		
(n = 9; size range, 15–27.1 cm dbh)		
Total biomass	$0.0939\times PV^{1.32}$	0.97
Leaf biomass	$0.0156\times PV-1.374$	0.94
Trunk biomass	$0.0175\times PV^{1.182}$	0.96
Branch biomass	$0.00000015\times PV^{3.103}$	0.96
Avicennia germinans		
(n = 7; size range, 14.2–26.3 cm dbh)		
Total biomass	$0.426\times PV^{1.062}$	0.99
Leaf biomass	$0.016\times PV^{1.027}$	0.95
Trunk biomass	$0.490\times PV^{1.009}$	0.99
Branch biomass	$0.000537\times PV^{1.792}$	0.96

Parabolic volume (dm^3) = $(1/2\times\pi\times r^2)\times$ height

were highly correlated (r = 0.98, $P < 0.001$ for surface water samples and r = 0.83, $P < 0.001$ for soil porewater samples). TP concentrations were significantly higher in the soil porewater than in the surface water (P = 0.001), but there were no significant differences among years (P = 0.20), nor any significant interaction between year and depth (P = 0.09). Surface water TP concentrations increased as surface water salinity decreased (r = −0.50, P = 0.02), but soil porewater TP concentrations were not correlated with salinity in either the surface water or soil porewater.

Soil concentrations of TP, reactive inorganic P, reactive organic P, and refractory organic P all increased with distance from the coast along transect 1 but remained constant across transect 2 (Figure 3d). Concentrations of Ca-P were greatest near the coast on transect 2 and were highest near the coast and in the plots most inland along transect 1. Average concentrations across all plots were as follows: TP = 15.1 ± 0.62 μMg^{-1}, reactive inorganic P = 2.4 ± 0.13 $\mu m\ g^{-1}$, reactive organic P = 5.8 ± 0.34 $\mu m\ g^{-1}$; Ca-P = 2.4 ± 0.34 $\mu m\ g^{-1}$, and refractory organic P = 4.5 ± 0.23 $\mu m\ g^{-1}$. Concentrations of reactive inorganic P were negatively correlated with surface water salinity (r = −0.61, P = 0.002) and porewater salinity (r = −0.61, P = 0.002) and positively associated with surface water PO_4^{3-} concentrations (r = 0.66, $P < 0.001$). All measured P pools except Ca-P pools were positively associated with surface water concentrations of TN ($P < 0.003$). Concentrations of both reactive and refractory organic P were negatively correlated with surface water salinity ($P < 0.001$).

Aboveground Biomass

Allometric relationships between tree parabolic volume and aboveground biomass components were all highly significant, with most r^2 values exceeding 0.95 (Table 1). Across the three species, 63%–83% of live biomass was allocated to the trunk, 10%–12.5% to branches, 3%–6% to twigs, 2%–4% to foliage, and 17% to prop roots (*R. mangle* only) (Table 2). *Rhizophora mangle* had the highest wood density (0.76 g m^{-3}), then *A. germinans* (0.64 g m^{-3}), then *L. racemosa* (0.60 g m^{-3}), but these differences were not significant ($F_{2,18}$ = 2.64, P = 0.10).

The mean aboveground biomass for the 23 plots was 233.5 ± 16.0 Mg ha^{-1} (range, 77.2–383.5) (Figure 2a). Across all the plots *A. germinans* comprised 9%, *L. racemosa* 34%, and *R. mangle* 57% of the total aboveground biomass measured in the plots at our study site. Sherman and others (1998) classified the 23 plots into the following four species assemblages: *R. mangle*–dominated (n = 12), *R.*

Table 2. Percentage of Dry Weight Allocated to the Biomass Components of Three Species of Mangrove Trees

	R. mangle (%)	*L. racemosa* (%)	*A. germinans* (%)
Trunk	63.10	81.00	82.80
Branches	10.40	12.50	11.30
Twigs	6.40	4.70	2.90
Leaf	2.90	1.80	3.00
Prop root	17.20		

mangle–L. racemosa mixed ($n = 4$), *L. racemosa*–dominated ($n = 4$), and *A. germinans*–dominated ($n = 3$) stands. Aboveground biomass was significantly different among stand types ($F_{3,22} = 11.25$, $P < 0.001$). Peak standing biomass was observed in the inland basin forest in stands dominated by *L. racemosa,* averaging 349.4 ± 12.3 Mg ha^{-1} dry weight, which was significantly greater than in the coastal sites dominated by *R. mangle* (195.4 ± 13.5 Mg ha^{-1}) and the more inland *A. germinans*–dominated stands (181.9 ± 57.0 Mg ha^{-1}). The mixed *R. mangle–L. racemosa* stands were intermediate (269.4 ± 6.8 Mg ha^{-1}). Although standing biomass was lowest near the inland forest margin in stands dominated by *A. germinans,* these two most inland plots exhibited signs of recent anthropogenic disturbance. In fact, some of our tagged trees were cut and removed from the forest. Hence, these plots were excluded from subsequent analyses.

Variation in aboveground biomass across the tidal gradient was negatively correlated with both surface water salinity ($r = 0.71$, $P < 0.001$) and soil porewater salinity ($r = 0.63$, $P = 0.02$), increasing linearly as salinity decreased (Figure 4a). Aboveground biomass increased linearly with TN concentrations in the surface water ($r = 0.44$, $P = 0.045$) and reactive inorganic P pools ($r = 0.54$, $P = 0.01$), but there were no other significant correlations between aboveground biomass and soil nutrients.

Leaf biomass did not differ significantly among stand types. *L. racemosa*–dominated stands averaged 7.3 ± 0.42 Mg ha^{-1}, *R. mangle–L. racemosa* mixed stands averaged 7.1 ± 0.97 Mg ha^{-1}, and *R. mangle*–dominated stands averaged 7.4 ± 0.45 Mg ha^{-1} ($F_{2,19} = 0.04$, $P = 0.957$) (Figure 2b). Surprisingly, leaf biomass showed only a weak trend with changing soil porewater salinity; being, slightly greater in the less saline plots ($r = 0.41$, $P = 0.066$), and it showed a weak positive linear relationship with TN concentrations in the surface water ($r = 0.41$, $P = 0.066$). Leaf biomass was positively correlated with concentrations of reactive organic P ($r = 0.64$, $P = 0.002$), refractory organic P ($r = 0.66$, $P = 0.001$), and TP ($r = 0.45$, $P = 0.04$) in the soil.

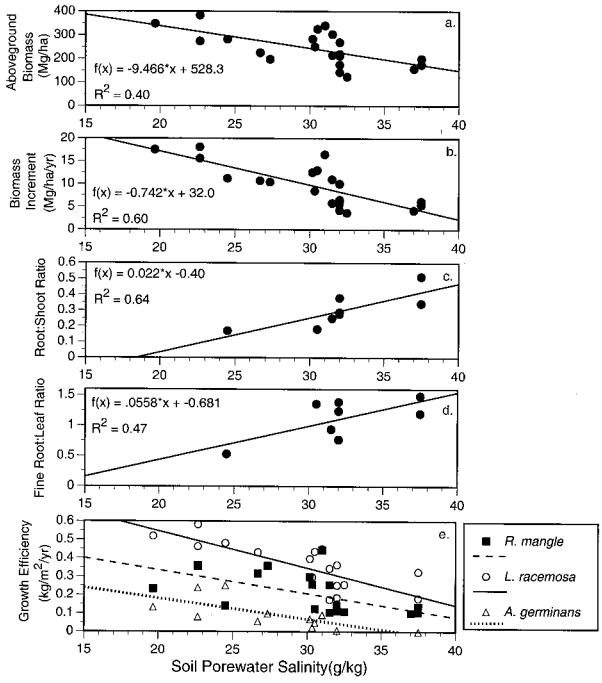

Figure 4. Changes in (a) aboveground biomass, (b) biomass increment, (c) root biomass (20 mm or less) to aboveground biomass, (d) fine-root biomass (2 mm or less) to leaf biomass ratios, (e) growth efficiency, and (f) relative rate of biomass increment for individual species measured in plots across a salinity gradient in a mangrove forest in the Dominican Republic. For a–d, each symbol represents a plot total. For e, each symbol represents an average value for each species by plot.

Spatial patterns of LAI across the tidal gradient were similar to those observed for leaf biomass ($r^2 = 0.96$, $P < 0.001$), with LAI ranging from 3.0 to 5.6 m^2 m^{-2} (Figure 2b). Area-to-weight ratios of *R. mangle* leaves (58.9 ± 1.2 cm^2 g^{-1}) and *L. racemosa* leaves (56.0 ± 1.6 cm^2 g^{-1}) were similar, whereas values for *A. germinans* leaves (107.0 ± 5.28 cm^2 g^{-1}) were significantly greater. Consequently, LAI did not differ significantly among stands dominated by either *R. mangle* or *L. racemosa* ($F_{2,19} = 0.24$, $P = 0.789$). LAI averaged 4.6 ± 0.22 in the *L. racemosa*–dominated stands, 4.2 ± 0.55 in the *R. mangle–L. racemosa* mixed stands, and 4.4 ± 0.26 in the *R. mangle*–dominated stands. There was a trend of increasing LAI with decreasing surface water salinity ($r = -0.44$, $P = 0.045$), increasing TN ($r = 0.47$, $P = 0.03$), total TP concentrations measured in the surface water ($r = 0.42$, $P = 0.06$), reactive organic

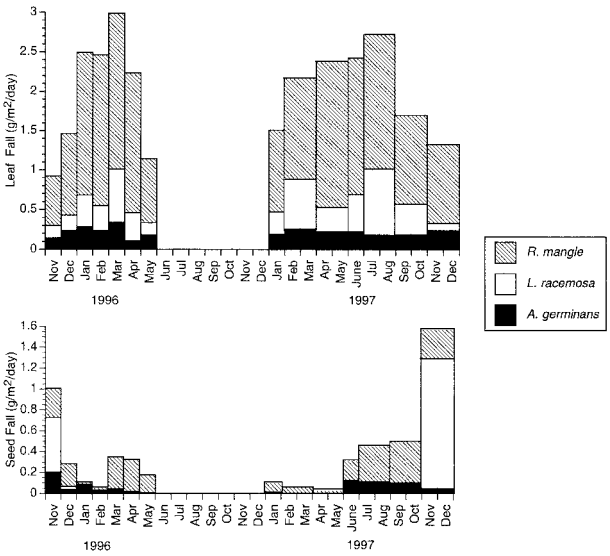

Figure 5. Seasonal patterns of leaf fall and seed fall measured in a mangrove forest over a 2-year period (1996–98). The width of the bar represents the time period over which collections were made; the overall height of the bar represents total litterfall for a given date. Segments represent individual species' contribution to the total.

P ($r = 0.70$, $P < 0.001$), refractory organic P ($r = 0.71$, $P < 0.001$), TP soil concentrations ($r = 0.57$, $P = 0.007$); but LAI was negatively associated with concentrations of Ca-P ($r = -0.67$, $P < 0.001$).

Litterfall

Daily rates of total litterfall averaged 3.13 g m^{-2} d^{-1} but varied significantly seasonally, ranging from 1.3 to 3.3 g m^{-2} d^{-1} between seasons ($F_{12,90} = 5.42$, $P < 0.001$) (Figure 5). There was a consistent seasonal pattern of decreased leaf fall during the winter months of November and December. Peak seed fall was also observed during this time. Leaves were the dominant component of litter throughout the year for all plots. Leaf litter contributed 64.9% of the total weight, reproductive tissues (flowers and seeds) accounted for 27.5%, and woody litter contributed 7.6%.

Total annual litterfall fluxes ranged from a low of 10.2 Mg ha^{-1} y^{-1} in the site nearest the coast to 12.8 Mg ha^{-1} y^{-1} in the more inland plots. Litterfall increased with decreasing salinity in both the surface water ($r = -0.87$, $P = 0.012$) and soil porewater ($r = -0.92$, $P = 0.004$) and increasing concentrations of reactive inorganic P ($r = 0.79$, $P = 0.015$) (Table 3). Total litterfall fluxes also showed a strong inverse relationship with NH_4^+ ($r = -0.85$, $P = 0.015$) (Table 3). However, leaf fall biomass had only a weak inverse relationship with soil porewater salinity ($r = -0.71$, $P = 0.07$) and was not associated with any other soil factor along the transect. Hence, turnover rates (ratio of leaf biomass to leaf litter flux) did not demonstrate any strong patterns across the salinity gradient. In contrast, seed deposition showed a strong linear increase across the transect with decreasing surface water salinity ($r = -0.87$, $P = 0.012$), NH_4^+ ($r = -0.95$, $P = 0.001$), and soil porewater salinity ($r = -0.78$, $P = 0.037$); seed deposition also showed a positive linear increase with TP concentrations in the surface water ($r = 0.81$, $P = 0.028$).

Table 3. Pearson Product Moment Correlation Coefficients between Soil Factors and Aboveground Net Primary Productivity (ANPP), Total Litterfall, and Seed Fall Measured in Permanent Plots in a Mangrove Forest in the Dominican Republic

Soil Factor	ANPP	Litterfall	Seed Fall
Surface water salinity	-0.779^{*}	-0.865^{*}	-0.865^{*}
Porewater salinity	-0.709	-0.915^{*}	-0.785^{*}
Surface water PO^{4-3}	0.882^{**}	0.565	0.809^{*}
Soil porewater $PO4^{-3}$	-0.084	-0.008	-0.096
Reactive P pools	0.814^{*}	0.792^{*}	0.705^{*}
Surface water $NH4^{*}$	-0.878^{**}	-0.853^{*}	-0.951^{**}

P, phosphorus
$^{*}P \leq 0.05$
$^{**}P \leq 0.01$

Biomass Increment

Annual biomass accumulation measured over the 4-y period (1994–98) averaged 9.7 ± 1.0 Mg ha^{-1} y^{-1} across all plots, ranging from 3.8 to 18.1 Mg ha^{-1} y^{-1} (Figure 2a). Spatial patterns of biomass increment across the tidal gradient paralleled those of total biomass ($r = 0.92$, $P < 0.001$). The annual biomass increment averaged 16.3 ± 1.1 Mg ha^{-1} y^{-1} in the *L. racemosa*–dominated stands, 11.8 ± 1.6 Mg ha^{-1} y^{-1} in the *L. racemosa–R. mangle* mixed stands, and 6.6 ± 0.75 Mg ha^{-1} y^{-1} in the *R. mangle*–dominated stands. Biomass increments in the *L. racemosa*–dominated and the *L. racemosa–R. mangle* mixed stands were not different, but they were significantly greater than the annual biomass increment of the *R. mangle*–dominated stands ($F_{2,19} = 21.46$, $P < 0.001$).

Spatial patterns of biomass increment across the intertidal gradient were strongly correlated with soil factors. Biomass increment decreased linearly with increases in surface water salinity ($r = -0.66$, $P = 0.001$) and soil porewater salinity ($r = -0.77$, $P < 0.001$). (Figure 4b).

Belowground Biomass

Fine-root biomass (2 mm or less) was more than 10 times greater in the solid peat than the intermediate soil substrate, and coarse-root biomass (2–20 mm) was more than three times greater. The proportion of substrate classified as solid peat decreased linearly with distance from the coast ($r = 0.89$, $P < 0.001$), whereas the intermediate substrate type increased ($r = 0.81$, $P = 0.005$), and the proportion of area as open water did not change ($r = 0.41$, $P = 0.181$). Across all 10 sites, the solid surface type accounted for 43.9% of the total area, the intermediate surface type amounted to 31.6%, and open water accounted for 24.4%.

Fine-root biomass (2 mm or less in diameter) ranged from 0.4 to 13.8 Mg ha^{-1}, with an overall mean of 7.9 ± 1.54 Mg ha^{-1} across the 10 plots. Fine-root biomass was substantially lower in the two most inland plots that had been partially cut over (0.6 Mg ha^{-1}) than in the undisturbed plots (average, 9.7 ± 1.21 Mg ha^{-1}, range, 2.9–13.8^{-1}); we therefore excluded these two disturbed sites from subsequent analysis. Coarse-root biomass (2–20 mm) was substantially higher than fine-root biomass, averaging 58.1 ± 5.8 Mg ha^{-1}. There was a linear trend of increasing root biomass with soil porewater salinity, but these relationships were not significant for fine-root biomass ($r = 0.64$, $P = 0.08$), coarse-root biomass ($r = 0.54$, $P = 0.17$), or total root (less than 20 mm) biomass ($r = 0.62$, $P = 0.10$). However, the ratio of total root biomass to aboveground biomass increased significantly with both surface water ($r = 0.76$, $P = 0.03$) and porewater salinity ($r = 0.80$, $P = 0.02$) (Figure 4c). The ratios of fine-root and coarse-root biomass to aboveground biomass also increased significantly with surface water (fine roots: $r = 0.74$, $P = 0.03$; coarse roots; $r = 0.72$, $P = 0.04$) and porewater salinity (fine roots: $r = 0.88$, $P = 0.004$; coarse roots: $r = 0.74$, $P = 0.04$). The ratio of fine-root biomass to leaf biomass also tended to increase with salinity, although the relationship was not significant ($r = 0.68$, $P = 0.06$) (Figure 4d). Root biomass was not significantly correlated with any other soil factors. Differences in root biomass among plots were not significantly correlated to any aboveground biomass components or productivity.

Aboveground Net Primary Productivity

Although we were able to calculate total aboveground net primary productivity (ANPP) for only seven of the plots, these plots were distributed across a range of salinities, so we were able to examine patterns in ANPP with respect to changing environmental factors. Total ANPP averaged 19.7 ± 1.46 Mg ha^{-1} y^{-1} and ranged from 15.6 to 25.0 Mg ha^{-1} y^{-1}. About 30% of aboveground production was allocated to stems, 7% to branch and twig production, 39% to leaf production, 20% to reproductive tissues, and 4% to prop root biomass. Total ANPP decreased with increasing surface water salinity ($r = -0.78$, $P = 0.04$) and NH_4^+ in the surface water ($r = -0.95$, $P = 0.001$), and it increased with increasing concentrations of TP in the surface water ($r = 0.88$, $P = 0.009$) and soil concentrations of reactive inorganic P ($r = 0.81$ $P = 0.03$) (Table 3). A weaker, linear trend was observed between ANPP and salinity in the soil porewater ($r = -0.71$, $P = 0.07$).

Growth Efficiency

Growth efficiency (ratio of aboveground biomass increment to LAI) (Waring 1983) decreased linearly with soil porewater salinity (r = -0.81, P<0.001), and showed a weaker, but significant negative relationships with surface water salinity (r=-0.45, P=0.045) and NH_4^+ concentrations (r=-0.50, P=0.02). The growth efficiency of individual species also decreased linearly with increasing soil porewater salinity (*R. mangle*: r=-0.56, P=0.009; *L. racemosa*: r=-0.75, P=0.009; *A. germinans*: r =-0.70, P=0.01; Figure 4e). The growth efficiency of *L. racemosa* (0.35±0.03 kg m^{-2} yr^{-1}) was significantly greater than *R. mangle* trees (0.21±0.02) which was significantly greater than *A. germinans* (0.09±0.02) ($F_{2,48}$=19.8, P<0.001). Consequently, the growth effiiciency of plots dominated by *L. racemosa* (0.36±0.02) was significantly greater than in *R. mangle*-dominated plots (0.17±0.03) and *R. mangle* -*L. racemosa* mixed plots (0.29±0.05) were intermediate ($F_{2,19}$=7.27, P=0.005). (*A. germinans*-dominated plots averaged 0.26±0.06 but were excluded from the analysis because of anthropogenic disturbance to these plots).

Discussion

Spatial variation in the biomass and net primary productivity of forest ecosystems has been attributed primarily to variations in climate and site fertility, as well as the disturbance history and age of forest stands (Ryan and others 1997; Barnes and others 1998). In an area of uniform climate and disturbance history, such as the Samaná Bay mangrove forest (Sherman and others 2000), variations in biomass and productivity should be attributed primarily to differences in soil factors, such as nutrient availability and salinity or other stressors. At

our study area, soil porewater salinity was strongly correlated with decreases in aboveground biomass, biomass increment, growth efficiency, and relative rates of biomass increment (Figure 4). Moreover, seed production and reproductive effort clearly declined with increasing salinity (Table 3). Hence, patterns of structural development and productivity along the tidal gradient at our site can probably be attributed to salinity or to some combination of salinity and other covarying environmental factors.

The cause–effect relationships between soil porewater salinity and forest biomass and productivity must remain tentative because, as has been noted by several authors (Patterson and Mendelssohn 1991; Smith 1992; McKee 1993; Upkong 1994), salinity often covaries with other potentially stressful factors in the soil environment, such as hydrogen sulfide concentrations, soil redox, and flooding frequency. However, in contrast to salinity, these environmental factors are difficult to quantify, whereas salinity provides a very straightforward and easily measurable index of stress. The high correlations between soil porewater salinity and forest biomass and productivity, although not conclusive evidence of cause and effect, provide a useful framework for field observations in complex mangrove landscapes where soil environmental stresses and resource availability may vary coincidentally. This problem in production ecology is intensified by the difficulties of reproducing these environmental complexes in controlled studies.

Hypersalinity has been implicated as a major factor limiting mangrove forest development (Lugo and others 1981), as have lower salinities such as those characteristic of our study area. For example, Imbert and others (2000) found a strong linear decrease in ANPP across a salinity gradient of 10–52 g kg^{-1} in *R. mangle* stands in Guadeloupe and Martinique. Saintilan (1997) documented decreases in the aboveground biomass of *Avicennia marina* and *Aegicera corniculatum* stands in an Australian mangrove forest across a salinity gradient that ranged from 5 to 50 g kg^{-1}. McKee and Faulkner (2000) found inverse correlations between leaf fall and salinity at levels below 50 g kg^{-1} in a Florida mangrove forest. These studies, together with our observations, suggest that moderate changes in salinity may inflict a physiological cost that alters the carbon (C) balance of mangrove trees, resulting in reductions in ANPP and biomass.

One component of this cost is suggested by the significant increases in the ratio of roots to shoots observed across the salinity gradient at our study site (Figure 4c). This result corresponds to those reported by Soto (1988) for *Avicennia germinans* growing across a salinity gradient that ranged from 35 to 85 g kg^{-1} in a Costa Rican mangrove. Similarly, Saintilan (1997) observed that root–shoot ratios increased along a salinity gradient of 5–50 g kg^{-1} and were significantly greater in hypersaline environments. Together, these results suggest that mangrove trees may allocate a greater proportion of C to belowground resources in more saline environments. This higher investment in roots probably contributes to the reduction in ANPP and growth efficiencies that we observed along the salinity gradient.

Experimental studies have shown that high salinity (Lin and Sternberg 1992), high soil sulfide concentrations (Lin and Sternberg 1992; McKee 1993), low soil redox potentials (McKee 1993; Pezeshki and others 1997), flooding conditions (Ellison and Farnsworth 1997), and low-nutrient conditions (Lin and Sternberg 1992; McKee 1995A) all can negatively affect mangrove seedling growth and, in some cases, increase C allocation to roots. Thus, it appears likely that other environmental stress factors are acting in combination with salinity to influence forest growth and productivity across the tidal gradient at our study site. Further research is needed to determine how mangrove species respond to various stress factors and how these responses influence mangrove forest dynamics.

The relationship between the tidal gradient and forest biomass and productivity is further complicated by coincident shifts in the species composition along the salinity gradient. The more saline sites near the coast with lower biomass and growth rates were dominated by *R mangle* whereas the more inland sites were dominated by *L. racemosa*. The high growth efficiency of *L. racemosa* as compared to the other two species, no doubt contributed to the higher biomass and productivity measured in sites dominated by this species. Somewhat surprisingly, the growth efficiency of all three mangrove tree species at our site decreased linearly as a function of increasing salinity even though the three species are thought to have very different tolerances to salinity (Smith 1992; Clough 1992). For example, even though *L. racemosa* is thought to be the least salt tolerant of the three species, it showed the greatest growth efficiency. Converesly, *A. germinans* appeared to be the most sensitive to the salinity even though this species is generally considered the most salt tolerant of the three species. Ball (1988) suggested that more salt tolerant species tend to grow more slowly than less tolerant species because of greater water use efficiences. Such interspecific differences in physiological responses to environ-

Table 4. Aboveground Biomass and Aboveground Net Primary Productivity of Worldwide Mangrove Forests

Study Site	Mangrove Type	Aboveground Biomass (Mg ha^{-1})	ANPP (Mg ha^{-1} y^{-1})	Salinity (g kg^{-1})	Age (y)	Reference
Neotropics						
Dominican Republic	Fringe	195.4	16.8[b]	33	50	Present study
Dominican Republic	Basin	349.4	23.6[b]	26	50	Present study
Florida	Fringe	56	8.8[b]	40	22	Warner 1990
Florida	Basin	72	8.8[b]	45	22	Warner 1990
Florida	Dwarf	22.3	8.1[b]	—	Mature	Ross and others 2001
Florida	Fringe	56.0	26.2[b]	—	8	Ross and others 2001
Guadeloupe	Scrub	47	6.1[b]	—	—	Imbert and Rollet 1989
Guadeloupe	Scrub	56	6.3[b]	—	—	Imbert and Rollet 1989
Guadeloupe	Fringe	99	21.2[b]	—	—	Imbert and Rollet 1989
Hawaii	Fringe	279	29.1[b]	15–55	—	Cox and Allan 1999
Mexico	Riverine	135	24.6[b]	0–5	—	Day and others 1987
Mexico	Fringe	120	16.1[b]	20–40	—	Day and others 1987
Puerto Rico	Fringe	62.9	12.4[b]	29	8	Golley and others 1962
Old World Tropics						
Indonesia	Fringe	93.7	20.8–25.0[b]	—	7	Sukardjo and Yamada 1992
Malaysia	Fringe	409	17.7[b]	—	86	Putz and Chan 1986
Malaysia	—	216.4[a]	24.5[b]	18	20	Ong and others 1995
Sri Lanka	Fringe	71	6.9[b]	29	—	Amarasinghe and Balasubramaniam 1992a, 1992b
Sri Lanka	Riverine	71	12.1[b]	5	—	Amarasinghe and Balasubramaniam 1992a, 1992b
Thailand	Fringe	159	27[b]	—	15	Christensen 1978
Western Australia	Fringe	246.7	75.6[a]	—	—	Alongi and others 2000
Western Australia	Fringe	45.8	46.9[c]	—	—	Alongi and others 2000
Australia	Riverine	711	45.4[d]	32	—	Clough 1992

ANPP, aboveground net primary productivity
[a]*Data were reported as t C ha^{-1} y^{-1}; we used a conversion factor of 2 to convert to total g dry weight.*
[b]*Estimated from measurements of biomass increment and litterfall*
[c]*Estimated from the light interception method*
[d]*Not reported*

mental conditions no doubt contribute to spatial patterns of mangrove forest biomass and growh.

The role of nutrient availability in regulating mangrove growth and productivity at our site is less clear because these patterns were not as strong as those related to porewater salinity and were somewhat inconsistent between the two transects. Fertilization studies (Boto and Wellington 1983; Feller 1995; Twilley 1995; Feller and others 1999) and comparative site studies (Boto and Wellington 1984; Chen and Twilley 1999) have indicated that P is the nutrient most limiting to plant growth in mangrove ecosystems. We observed a strong relationship between increasing ANPP and soil solution P, although it occurred across a limited section of the transect; moreover, aboveground biomass was positively correlated with concentrations of reactive inorganic soil P. These findings suggest that P plays a role in regulating the patterns of forest growth at this site. However, we also found strong positive correlations between concentrations of organic soil P and leaf biomass and LAI that suggest a plant effect on the soil chemistry pools. Although the more nutrient-rich environments of the inland sites probably contributed to the higher biomass and productivity, untangling the relative influences would require fertilization experiments and more dynamic measurements of nutrient mineralization and flux.

The possibility that more efficient recycling of limiting nutrients plays a role regulating productivity patterns should also be acknowledged. We found evidence that decomposition rates were higher in the more inland plots at our site (Sherman and others 1998). These findings support the observations of Twilley and others (1986) that in-

land basin mangroves have higher internal recycling rates of nutrients from litter on the forest floor. Moreover, the leaves of *L. racemosa* and *A. germinans*, the dominant species of inland basin forests, have lower C:N and C:P ratios than *R. mangle* leaves, which enhances decomposition rates (Twilley and others 1986; Sherman and others 1998). Such a feedback could reinforce plant–soil relationships and contribute to patterns of mangrove growth and development.

The nutrient concentrations measured at our study site are typical of mangrove ecosystems. Concentrations of dissolved inorganic P in mangroves typically are less than 40 $\mu M\ L^{-1}$ (Clough 1992) and often less than 2 $\mu M\ L^{-1}$ (Chen and Twilley 1999). NH_4^+ typically is the dominant inorganic N species; concentrations have been reported to range from 0 to 760 $\mu M\ L^{-1}$. The negative relationship between NH_4^+ and ANPP observed at our site may be explained by the influence of salinity on soil exchange processes. Salinity and NH_4^+ were positively correlated, suggesting that sodium ions were replacing NH_4^+ on the soil exchange complex.

Globally, the aboveground biomass of mangrove forests has been reported to range from 6.8 to 436.4 Mg ha^{-1} (Saenger and Snedaker 1993), estimated litterfall ranges from 1.3 to 18.7 Mg $ha^{-1}\ y^{-1}$ (Saenger and Snedaker 1993), and ANPP ranges from 6.9 to 75.6 Mg $ha^{-1}\ y^{-1}$ (Table 4). Compared to global values, values at our site were at the upper end of the range. Saenger and Snedaker (1993) compiled global data on mangrove forests and developed a regression model to predict biomass and litterfall from latitude and canopy height. The model predicted a biomass of 172 Mg ha^{-1} and litterfall rates of 10.8 Mg $ha^{-1}\ y^{-1}$ for the Samaná Bay mangrove; hence, biomass (233.5 Mg ha) was underestimated by the model, and litterfall (11.4 Mg ha y^{-1}) was predicted accurately. Saenger and Snedaker (1993) suggested that, at a given latitude, high values for biomass and litterfall indicate optimum growing habitats, such as low salinity, high fertility, and favorable climatic conditions. The location of the Samaná Bay mangrove forest, in a humid climate and in the deltas of two rivers, places it in a potentially highly productive zone. However, because biomass is also highly dependent upon stand age, the high biomass of the Samaná Bay mangrove can be partially attributed to its relatively mature age (more than 50 years old).

Compared with global mangrove forests, the LAI at the Samaná Bay mangrove (average, 4.4 $m^2\ m^{-2}$) is intermediate. LAI ranged from 2.2 to 7.4 (average, 4.9) for a wide range of mangrove forests in Thailand, Malaysia, and northern Australia (Cheeseman and others 1991; Clough 1992). The LAI of dwarf forests in Florida can range from less than 1 to 3, whereas the LAI for basin and riverine forests ranges from 5 to 6 (Lugo and others 1975; Lugo and Patterson-Zucca 1977; Pool and others 1977; Araujo and others 1997). The range was 3.3–4.9 for different-aged *R. apiculata* stands in Vietnam (Clough and others 1999) and 4.4–5.1 for *R. apiculata* stands in Malaysia (Clough and others 1997).

Our ability to document strong spatial patterns that suggested environmental controls on forest biomass and growth stems from the fact that the area was mostly even-aged, having arisen following a tidal wave that destroyed much of the forest in 1946 (Sherman and others 2000). Because forest biomass and ANPP are strongly dependent upon stand age (Ryan and others 1997), it would be difficult to demonstrate patterns in relation to the environmental gradient in sites with a more complex disturbance history. In September 1998, our site was damaged extensively by Hurricane Georges, the first major disturbance since the 1946 tidal wave. Surveys of our permanent plots indicated that approximately 42% of the forest biomass was killed. Patterns of damage were spatially heterogeneous, and standing biomass was reduced from 9%–100% in the different plots (Sherman and others 2001). The recovering forest will consist of a patchwork of stands that originated in 1946 and 1998, as well as stands composed of a mix of these two age classes. Thus, interpreting productivity patterns will be more complicated. However, future research can capitalize on this disturbance by identifying changes in biomass, productivity, and biogeochemistry during forest development as it recovers from this large-scale disturbance.

REFERENCES

Alongi DM, Tirendi F, Clough BF. 2000. Below-ground decomposition of organic matter in forests of the mangrove *Rhizophora stylosa* and *Avicennia marina* along the arid coast of western Australia. Aquat Bot 68:97–122.

Alvarez V, Cintrón G. 1984. Los manglares de la Republica Dominicana. Numero 53:1–23.

Amarasinghe MD, Balasubramianiam S. 1992. Net primary productivity of two mangrove forest stands on the northwestern coast of Sri Lanka. Hydrobiologia 247a:37–47.

Amarasinghe MD, Balasubramianiam S. 1992. Structural properties of two types of mangrove stands on the northwestern coast of Sri Lanka. Hydrobiologia 247b:17–27.

Araujo RJ, Jaramillo JC, Snedaker SC. 1997. LAI and leaf size differences in two red mangrove forest types in South Florida. Bull Mar Sci 60:643–7.

Ball MC. 1988. Salinity tolerance in the mangroves *Aegiceras corniculatum* and *Avicennia marina*. I. Water use in relation to growth, carbon partitioning, and salt balance. Aust J Plant Physiol 15:447–64.

Barnes BV, Zak, DR, Denton SR, Spurr SH. 1998. Forest ecology. 4th ed. New York: Wiley. 774 p.

Boto KG, Wellington JT. 1983. Phosphorus and nitrogen nutritional status of a northern Australian mangrove forest. Mar Ecol Progr Ser 11:63–9.

Boto KG, Wellington JT. 1984. Soil characteristics and nutrient status in a northern Australian mangrove forest. Estuaries 1:61–9.

Canfield RH. 1941. Application of the line interception method in sampling range vegetation. J For 39:388–94.

Carpenter SR, Turner MG. 1998. At last. Ecosystems 1:1–5.

Cheeseman JM, Clough BF, Carter DR, Lovelock CE, Ong JE, Sim RG. 1991. The analysis of photosynthetic performance in leaves under field conditions. Photosyn Res 29:11–22.

Chen R, Twilley RR. 1999. Patterns of mangrove forest structure and soil nutrient dynamics along the Shark River estuary, Florida. Estuaries 22:955–70.

Christensen B. 1978. Biomass and productivity of *Rhizophora apiculata* B1. in a mangrove in southern Thailand. Aquat Bot 4:43–52.

Clough B, Tan DT, Phuong DX, Buu DC. 1999. Canopy leaf area index and litter fall in stands of the mangrove *Rhizophora apiculata* of different age in the Mekong delta, Vietnam. Aquat Bot 66:311–20.

Clough BF. 1992. Primary productivity and growth of mangrove forests. In: Robertson AI, Alongi DM, editors. Tropical mangrove ecosystems. Washington (DC): American Geophysical Union. p 225–50.

Clough BF, Ong JE, Gong WK. 1997. Estimating leaf area index and photosynthetic production in canopies of the mangrove *Rhizophora apiculata.* Mar Ecol Prog Ser 159:285–92.

Cox EF, Allen JA. 1999. Stand structure and productivity of the introduced *Rhizophora mangle* in Hawaii. Estuaries 22:276–84.

Day JW, Conner WH, Ley LF, Day RH, Navarro AM. 1987. The productivity and composition of mangrove forests, Laguna de Terminos, Mexico. Aquat Bot 27:267–84.

Ellison AM, Farnsworth EJ. 1993. Seedling survivorship, growth, and response to disturbance in Belizean mangal. Am J Bot 80:1137–45.

Ellison AM, Farnsworth EJ. 1997. Simulated sea level change alters anatomy, physiology, growth, and reproduction of red mangrove (*Rhizophora mangle* L.). Oecologia 112:435–46.

Feller IC. 1995. Effects of nutrient enrichment on growth and herbivory of dwarf red mangrove (*Rhizophora mangle*). Ecol Monogr 65:477–505.

Feller IC, Whigham DF, O'Neill JP, McKee KL. 1999. Effects of nutrient enrichment on within-stand cycling in a mangrove forest. Ecology 80:2193–205.

Golley F, Odum HT, Wilson R. 1962. The structure and metabolism of a Puerto Rican red mangrove forest in May. Ecology 43:9–19.

Grasshoff K, Ehrhardt M, Kremling K. 1983. Methods of seawater analysis. 2nd ed. Weinhein (Germany): Verlag Chemie. 419 p.

Hughes JW, Fahey TJ, Browne B. 1987. A better seed and litter trap. Can J For Res 17:1623–1624.

Jensen HS, Thamdrup B. 1993. Iron-bound phosphorus in marine sediments as measured by bicarbonate-dithionite extraction. Hydrobiologia 253:47–59.

Imbert D, Rollet B. 1989. Phytomasse aerienne et production primaire dans la mangrove du Grand Cul-de-Sac Marin (Guadeloupe, Antilles Françaises). Bull Ecol 20:27–39.

Imbert D, Rousteau A, Scherrer P. 2000. Ecology of mangrove growth and recovery in the Lesser Antilles. Restor Ecol 8:230–6.

Lin G, Sternberg LDL. 1992. Effects of growth form, salinity, nutrient and sulfide on photosynthesis, carbon isotope discrimination and growth of red mangrove (*Rhizophora mangle* L.). Aust J Plant Physiol 19:509–17.

Lugo AE, Cintron G, Goenaga C. 1981. Mangrove ecosystems under stress. In: Barrett GW, Rosenberg R, editors. Stress effects on natural ecosystems. Chichester (UK): J Wiley. p 129–54.

Lugo AE, Evink G, Brinson MM, Broce A, Snedaker SC. 1975. Diurnal rates of photosynthesis, respiration and transpiration in mangrove forests of South Florida. In: Golly FB, Medina E, editors. Tropical ecological systems. New York: Springer-Verlag. p 335–50.

Lugo AE, Patterson-Zucca C. 1977. The impact of low temperature stress on mangrove structure and growth. Tropic Ecol 18:149–61.

McKee KL. (1995a) Interspecific variation in growth, biomass partitioning, and defensive characteristics of neotropical mangrove seedlings: response to light and nutrient availability. AM J Bot 82:299–307.

McKee KL. 1995b. Seedling recruitment patterns in a Belizean mangrove forest. Oecologia 101:448–60.

McKee KL. 1993. Soil physicochemical patterns and mangrove species distribution—reciprocal effects? J Ecol 81:477–87.

McKee KL, Faulkner PL. 2000. Restoration of biogeochemical function in mangrove forests. Restor Ecol 8:247–59.

Ong J-E, Gong WK, Clough BF. 1995. Structure and productivity of a 20-year-old stand of *Rhizophora apiculata* B1. mangrove forest. J Biogeog 22:417–24.

Pasch RJ. 1999. Atlantic hurricanes. Weatherwise 52:48–53.

Patterson CS, Mendelssohn IA. 1991. A comparison of physicochemical variables across plant zones in a mangal/saltmarsh community in Louisiana. Wetlands 11:139–59.

Pezeshki SR, DeLaune RD, Meeder JF. 1997. Carbon assimilation and biomass partitioning in *Avicennia germinans* and *Rhizophora mangle* seedlings in response to soil redox conditions. Environ Exp Bot 37:161–71.

Pool DJ, Snedaker SC, Lugo AE. 1977. Structure of mangrove forests in Florida USA, Puerto Rico, Mexico, and Coast Rica. Biotropica 9:195–212.

Putz F, Chan HT. 1986. Tree growth, dynamics, and productivity in a mature mangrove forest in Malaysia. For Ecol Manage 17:211–30.

Ross MS, Ruiz PL, Telesnicki GJ, Meeder JF. 2001. Estimating above-ground biomass and production in mangrove communities of Biscayne National Park, Florida (USA). Wetlands Ecol Manage 9:27–37.

Ryan M, Binkley D, Fownes J. 1997. Age-related decline in forest productivity. Adv Ecol Res 27:213–62.

Sachtler ML. 1973. Inventario y fomento de los recursos forestales: Republica Dominicana Inventario Forestal. Informe Technico 3. Santo Domingo: FAO.

Saenger P, Snedaker SC. 1993. Pantropical trends in mangrove above-ground biomass and annual litterfall. Oecologia 96:293–9.

Saintilan N. 1997. Above- and below-ground biomasses of two

species of mangrove on the Hawkesbury River estuary, New South Wales. Mar Freshwater Res 48:147–52.

Sherman RE, Fahey TJ, Battles JJ. 2000. Small-scale disturbance and regeneration dynamics in a neotropical mangrove forest. J Ecol 88:165–78.

Sherman RE, Fahey TJ, Howarth RW. 1998. Soil–plant interactions in a neotropical mangrove forest. Oecologia 115:553–63.

Sherman RE, Fahey TJ, Martinez P. 2001. Hurricane impacts on a mangrove forest in the Dominican Republic. Biotropica 33: 393–401.

Smith TJ III. 1992. Forest structure. In: Robertson AI, Alongi DM, editors. Tropical mangrove recosystems. Washington (DC): American Geophysical Union. p 101–36.

Soto R. 1988. Geometry, biomass allocation, and leaf life-span of *Avicennia germinans* (L.) L. (Avicenniaceae) along a salinty gradient in Salinas, Puntarenas, Costa Rica. Rev Biol Tropic 36:309–23.

Sukardjo S, Yamada I. 1992. Biomass and productivity of a *Rhizophora mucronata* Lamarck plantation in Tritih, Central Java, Indonesia. For Ecol Manage 49:195–209.

Thom BG. 1967. Mangrove ecology and deltaic geomorphology: Tabasca, Mexico. J Ecol 55:301–43.

Thom BG. 1982. Mangrove ecology—a geomorphological perspective. In: Clough BF., editor. Mangrove ecosystems in Australia. Canberra: Australian University Press. p 3–17.

Twilley RR. 1995. Properties of mangrove ecosystems related to the energy signature of coastal environments. In: Hall CS, editor. Maximum power. Boulder (CO): University of Colorado Press. p 43–62.

Twilley RR, Lugo AE, Patterson-Zucca C. 1986. Litter production and turnover in basin mangrove forests in southwest Florida. Ecology 67:670–83.

Upkong IE. 1994. Soil–vegetation interrelationships of mangrove swamps as revealed by multivariate analysis. Geoderma 64: 167–81.

Waring RH. 1983. Estimating forest growth and efficiency in relation to canopy leaf area. Adv Ecol Res 13:327–54.

Warner JH. 1990. Successional patterns in a mangrove forest in southwest Florida [thesis]. University of Southwestern Lousianna, p 49.

Whittaker RH, Bormann FH, Likens GE, Siccama TG. 1974. The Hubbard Brook ecosystem study. Ecol Monogr 44:233–54.

Whittaker RH, Woodwell GM. 1968. Dimension and production relations of trees and shrubs in the Brookhaven Forest, New York. J Ecol 56:1–25.

Wolanski E, Mazda Y, Ridd P. 1992. Mangrove hydrodynamics. In: Robertson AI, Alongi DM, editors. Tropical mangrove ecosystems. Washington (DC): American Geophysical Union. p 43–62.

Woodroffe C. 1992. Mangrove sediments and geomorphology. In: Robertson AI, Alongi DM, editors. Tropical mangrove ecosystems. Washington (DC): American Geophysical Union. p 7–42.